Ionization of molecules by multicharged bared ions by using the stoichiometric model

author

Instituto de Astronomía y Física del Espacio
(CONICET-UBA). Casilla de correo 67, sucursal 28
(C1428EGA) Buenos Aires, Argentina.

September 6, 2019

Abstract

1 Introduction

The damage caused by the impact of multicharged heavy projectiles has become a field of interest due to its recent implementation in ion-beam cancer therapy. The effectiveness of the radiation depends on the choice of the ions. In particular, theoretical and experimental studies with different projectiles have concluded that charged carbon ions could be the most suitable ions to use. The study of such systems represent a challenge from the theoretical point of view. The most widely used method to compute ionization of multicharged atoms is the first Born approximation. This perturbative method warrants the Z^2 laws, where Z is the projectile charge. However, the damage concentrated in the vicinities of the Bragg peak correspond to energies of hundreds of KeV/amu. Precisely in this region, often refered to as the intermediate energy region, the Born approximation starts to fail. Another theoretical issue arises from the targets themselves; we are dealing with complex molecules. This article deals precisely with these two aspects. First, we

perform more appropriate calculations on the primary damage mechanism, i.e., atomic ionization by multicharged ions, which can replace the Born results. Second, we inspect and use an stoichiometric model, which reduces a molecule to a sum of atomic processes quantities weighted by the number of such atom in the molecule.

To overcome the first perturbative approximation limitations, and since the projectiles are multicharged ions, we resort to the Continuum Distorted Wave-Eikonal Initial State (CDW), which includes higher perturbative corrections. We start from the premise that the ionization process is the mechanism that deposits the most significant amount of primary energy. This process produces an electron-energy spectrum that needs to be integrated. Moreover, the ejected electrons become a new source of local damage. These secondary electrons are included in Monte Carlo simulations and hence their behavior must be investigated. With this end in mind, we calculate not only the ionization cross-sections but also energy and mean angular distributions of the emitted electrons.

The molecular structure complexity of the target is dealt with by implementing the simplest stoichiometric model (SSM); we assume that the molecule is composed of isolated independent atoms. In all cases, the total cross-section is simply the sum of the cross-section of each atom.

Then, by implementing the SSM and the CDW –instead of the first Born approximation–, we calculate ionization cross-section of several molecules (see Table 1) by the impact of antiprotons, H^+, He^{2+}, Be^{4+}, C^{6+}, and O^{8+}. Furthermore, in Section 3, we investigate different DNA and RNA molecules such as adenine, cytosine, guanine, thymine, uracil, and also DNA backbone.

The results are processed to test the Toburen scaling rule, which states that the ratio between the ionization cross-section and the number of valence electrons (outer electrons) in terms of the projectile velocity can be arranged in a narrow universal band. We have also applied this rule to several hydrocarbons and nucleobases. In Section 3.2, we will prove that the width of the resulting universal band can be significantly reduced if we redefine the effective number of valence electrons.

It is well known that the residual electrons from the ionization process cause significant biological damage. To inspect this mechanism, in Section 3.3 and 3.4, we calculated the mean electron energy and angular distributions. Surprisingly, we found a substantial dependence of the charged projectile, which is unexpected in the first Born approximation.

The hefty charge projectiles are dealt with the CDW. However, the stoi-

chiometric model used seems to be very simplistic. The approximation considers each atom as neutral, which is not correct. In Section 3.5, we used the molecular electronic structure code GAMESS [1] to calculate the excess or defect of electron density one each atom. Then, the simple stoichiometric model is modified to account for the departure from neutrality of the atoms. We find that for the DNA molecules this modification does not introduce a substantial change.

2   Theory: Ionization of Atoms

In our study, we will consider six atoms α = H, C, N, O, P, and S. Most of the organic molecules are composed of these atoms. Some particular molecules also include halogen atoms such as fluor and bromine; ionization cross-sections of these elements have been previously published [2, 3].

The total ionization cross-sections of these atoms were calculated using the CDW. The initial bound and final continuum radial wave functions were obtained by using the RADIALF code, developed by Salvat and co-workers, and a Hartree-Fock potential obtained from the Depurated Inversion Model [4, 5]. We used a few thousand pivot points to solve the Schrödinger equation, depending on the number of oscillations of the continuum state. The radial integration was performed using the cubic spline technique. The number of angular momenta considered varied from 8, at very low ejected-electron energies, up to 30, for the highest energies considered. The same number of azimuth angles were required to obtain the four-fold differential cross-section. The calculation performed does not display prior-post discrepancies at all. Each atomic total cross-section in Eq. (1) was calculated using 35 to 100 momentum transfer values, 28 fixed electron angles, and around 45 electron energies depending on the projectile impact energy. Further details of the calculation are given in Ref. [6]. Simultaneously, we will be reporting state to state ionization cross sections for these cases in Ref. [7], which will be very useful to estimate molecule fragmentation.

In Figure 1, we report our total ionization results for the six essential elements by the impact of six different projectiles: antiprotons, H^+, He^{2+}, Be^{4+}, C^{6+}, and O^{8+}. To reduce the resulting 36 magnitudes into a single consistent figure, we considered the fact that in the first Born approximation the ionization cross-section scales with the square of the projectile charge, Z^2. The values of the impact energies considered range between 0.1 to 10

CH	CH$_4$, C$_2$H$_2$, C$_2$H$_4$, C$_2$H$_6$, and C$_6$H$_6$
CHN	C$_5$H$_5$N, C$_4$H$_4$N$_2$, C$_2$H$_7$N, and CH$_5$N
DNA	adenine (C$_5$H$_5$N$_5$), cytosine (C$_4$H$_5$N$_2$O), guanine (C$_5$H$_5$N$_5$O), thymine (C$_5$H$_6$N$_2$O$_2$), uracil (C$_4$H$_4$N$_2$O$_2$), DNA backbone (C$_5$H$_{10}$O$_5$P), dry DNA (C$_{20}$H$_{27}$N$_7$O$_{13}$P$_2$)

Table 1: Sixteen molecular targets of our interest classified in three families.

MeV/amu, where the CDW is supposed to hold. In fact, for the highest projectile charges the minimum impact energy where the CDW is expected to be valid could be higher than 100 KeV. Moreover, we corroborated that the first Born approximation provides quite reliable results only for energies higher than a couple of MeV/amu. We use the same color to indicate the projectile charge throughout the figures of this work: dashed-red, solid-red, blue, magenta, olive and orange for antiprotons, H$^+$, He^{2+}, Be^{4+}, C^{6+}, and O^{8+}, respectively. Notably, there is no complete tabulation of ionization of atoms by the impact of multicharged ions. We hope that the ones presented in this article will be of help for future works.

3   Ionization of Molecules

3.1   The stoichiometric model

Lets us consider a molecule M composed by n_α atoms of the element α, the SSM describes the total ionization cross section of the molecule σ_M as a simple sum of ionization cross sections of the isolated atoms σ_α,

$$\sigma_M = \sum_\alpha n_\alpha \sigma_\alpha . \tag{1}$$

We divided sixteen molecular targets of our interest in three families. The classification defined is given in Table 1.

In Figure 2, we report the total ionization cross sections by the impact of multicharged ions for the four fundamental DNA components: adenine, cytosine, guanine and thymine. Our reports for uracil and DNA backbone containing P are given in Figure 3. For adenine, the agreement with the

experimental data available in our range of validity is quite good. For uracil, we have a puzzling situation: our results show good agreement with the experiments by proton impact of Itoh *et al.* [8], but for the same target our theory fails by a factor of two for the impact of C^{4+} and O^{6+} ions. Nonetheless, it should be stated that our theoretical results coincide with calculations by Champion, Rivarola and collaborators [10, 11], which may indicate a possible misstep of the experiments.

3.2 Scaling rule

The first attempt to develop a comprehensive but straightforward phenomenological model for electron ejection from large molecules was proposed by Toburen *et al.* [12, 13]. The authors found it convenient to scale the experimental ionization cross section in terms of the number of outer or weakly bound valence electrons (total number of electrons minus the inner-shell ones). We introduce the cross section per weakly bound electron or ionization cross section per valence electron, σ_e, as

$$\sigma_e = \frac{\sigma_M}{N_M} = \frac{\sum\limits_{\alpha} n_\alpha \sigma_\alpha}{\sum\limits_{\alpha} n_\alpha \nu_\alpha} = \sigma_e(v) \,, \tag{2}$$

where

$$\nu_\alpha = \left\{ \begin{array}{ll} 4, & \text{for C,} \\ 5, & \text{for N and P,} \\ 6, & \text{for O and S,} \end{array} \right. \tag{3}$$

and $\nu_H = 1$. The Toburen rule can be stated by saying that σ_e is a *universal* parameter independent on the molecule, which depends solely on the impact velocity. In Ref. [13], it was found experimentally that for proton impact on some simple molecules, σ_e results

$$\begin{array}{llll} E(\text{MeV}) & 0.25 & 1.00 & 2.00 \\ \sigma_e(10^{-16} cm^2) & 0.39 & 0.17 & 0.11 \end{array} \tag{4}$$

with an estimated error of about 20%. A similar ratio was found in Ref. [8] for proton impact on uracil and adenine. Figure 4a shows σ_e calculated with the CDW as a function of the impact velocity for different projectile charges computed with the SSM for the sixteen molecular targets displayed in Table 1. The universality with Z is the one provided by Born approximation,

i.e., $\sigma_e(Z) = Z^2 \sigma_e(Z=1)$, and it holds for large impact velocities, as shown Figure 4a. Of course, for lower impact velocities, the CDW breaks the behavior of the Z^2 rule. Although the Toburen rule holds for high energies, its performance is still not satisfactory: the universal band is quite broad. The departure of our theoretical results from the Toburen rule can be easily explained by the fact that our atomic cross sections σ_α behave differently for each atom in terms of the projectile charges. By inspecting Figure 1, one can easily see that the rule $\sigma_\alpha / \nu_\alpha \sim \sigma_e$ is not well satisfied by the CDW. A much better general atomic rule is given by

$$\sigma_e^{\text{CDW}} = \frac{\sum\limits_\alpha n_\alpha \sigma_\alpha^{\text{CDW}}}{\sum\limits_\alpha n_\alpha \nu_\alpha^{\text{CDW}}}, \tag{5}$$

where

$$\nu_\alpha^{\text{CDW}} \sim \begin{cases} 4, & \text{for C, N, and O,} \\ 4.5, & \text{for P and S} \end{cases} \tag{6}$$

and, obviously, $\nu_{\text{H}}^{\text{CDW}} = 1$. The cross sections σ_e^{CDW} are plotted in Figure 4b. A much better sharp band is observed, especially at high energy, where the theory is expected to work. It will be interesting for experiments to cross-check this theoretical prediction.

3.3 Emitted electron energies

In a given biological medium, direct ionization by ion impact accounts for just a fraction of the overall damage. Secondary electrons, as well as recoil target ions, also contribute substantially to the total damage. We can consider the single differential cross section of the shell nl of the atom α, $d\sigma_{\alpha nl}/dE$, to be a function of the ejected electron energy E as a simple distribution function [14]. Then, we can define the mean value $\overline{E}_\alpha$ as in Ref. [15],

$$\overline{E}_\alpha = \frac{\langle E_\alpha \rangle}{\langle 1 \rangle} = \frac{1}{\sigma_\alpha} \sum_{nl} \int dE\, E \frac{d\sigma_{\alpha,nl}}{dE}, \tag{7}$$

$$\langle 1 \rangle = \sigma_\alpha = \sum_{nl} \int dE\, \frac{d\sigma_{\alpha,nl}}{dE}, \tag{8}$$

where Σ_{nl} takes into account the sum of the different sub-shell contributions of the element α.

Figure 5 shows $\overline{E}_\alpha$ for six elements from Table 1. The range of impact velocities was shorten up to $v = 10$ a.u. due to numerical limitations in the spherical harmonics expansion. In our theoretical treatment, we expand our final continuum wave function as per usual,

$$\psi_{\overrightarrow{k}}^-(\overrightarrow{r}) = \sum_{l=0}^{l_{\max}} \sum_{m=-l}^{l} R_{kl}^-(r) Y_l^m(\widehat{r}) Y_l^{m*}(\widehat{k}) . \tag{9}$$

We are confident with our calculations up to $l_{\max} \sim 30$. As the impact velocity v increases, so do $\langle E_\alpha \rangle$ and $l_{\max}$, which results in the inclusion of very oscillatory functions in the integrand. Furthermore, the integrand of $\langle E_\alpha \rangle$ includes the kinetic energy E (see Eq. (7)), which cancels the small energy region and reinforces the large values, making the result more sensible to large angular momenta. Regardless, for $v > 10$ a.u., the first Born approximation holds.

In Figure 5, we estimate $\overline{E}_\alpha$ in the 0.5–2 a.u. velocity range, or equivalently from 15 to 50 eV, for all the targets. Our results agree with the experimental findings [14]. The dependence of the mean energy value with the projectile charge Z is surprisingly sensible, which can duplicate the proton results. This effect can be attributed to the depletion caused by the multicharged ions to the yields of low energy electrons. In the high electron energy regime, the CDW falls on the simple first Born approximation, surviving the Z^2 law. Then, the ratio in Eq. (7) cancels out and $\overline{E}_\alpha$ becomes a universal value independent on Z.

Extending the simple stoichiometric model for the mean electron energy calculation, it results

$$\overline{E}_M = \frac{\sum\limits_\alpha n_\alpha \overline{E}_\alpha}{\sum\limits_\alpha n_\alpha \sigma_\alpha} . \tag{10}$$

For impact of H^+ and He^{2+} on water at 1 MeV/amu, we obtain $\overline{E}_{H_2O} = 43.7$ and 45 eV, while the experimental values on liquid water by Pimblott and LaVerne [xxx] were found to be 51.5 and 52.2 eV, respectively. Just to stress the importance of the projectile charge, for O^{8+} on water, at the same impact energy 1 MeV/amu, we obtained $\overline{E}_{H_2O} = 54.7$ eV, which is 25% larger than proton impact result. It is worth noting that there should not be any difference if the calculations were carried in first Born approximation. We will came back on this issue later.

3.4 Emitted electron angles

As mentioned before, secondary electrons contribute to the total damage. Then, not only is the ejection energy important but also the angle of emission. Once again, we can consider the single differential cross section in terms of the ejected electron solid angle Ω, $d\sigma_{\alpha,nl}/d\Omega$, to be expressed as a distribution function, and the mean angle $\bar{\theta}_\alpha$ can be defined as

$$\bar{\theta}_\alpha = \frac{\langle \theta_\alpha \rangle}{\langle 1 \rangle} = \frac{1}{\sigma_\alpha} \sum_{nl} \int d\Omega\, \theta\, \frac{d\sigma_{\alpha,nl}}{d\Omega} \tag{11}$$

Figure 6 shows $\bar{\theta}_\alpha$ for our six elements of interest. A new important dependence of $\bar{\theta}_\alpha$ with Z is observed. It is a general belief [21] that the angular dispersion of emitted electrons are nearly isotropic. This effect is caused by the insignificant angular anisotropy of sub-50-eV yield. A typical value for the ejection angle considered in the literature is $\bar{\theta}_\alpha \sim 70°$ [14], and it is quite correct in the range of validity of the first Born approximation for any target. But, when a distorted wave approximation is used, $\bar{\theta}_\alpha$ decreases substantially with Z in the intermediate energy region, as observed in Figure 6. For example, for C^{6+} impact, the Bragg peak occurs at 0.3 MeV/amu, where $\bar{\theta}_\alpha$, computed with the CDW method, is about half of the value obtained with the first Born approximation. This correction should close the damage to the forward direction.

We can attribute this correction to the capture to the continuum effect; the larger the charge Z, the smaller $\bar{\theta}$ will be. Of course, this effect only holds at intermediate energies and not at high impact energies, where the Born approximation rules. One illustrative observation is the behavior of antiprotons: the projectile in this case repels the electrons, making the distribution almost symmetric. Note the opposite effect of proton and antiprotons; they run one opposite to the other, as compared with the first Born approximation.

3.5 A modified stoichiometric model

The SSM considers the molecule to be assembled by isolated neutral atoms, which is definitively unrealistic. A first improvement can be suggested by assuming that the atoms are not neutral and that they have an uneven distribution of electrons within the molecule; this distribution can be given by an effective charge q_α. A possible value for q_α is given by the Mulliken charge.

8

However, there are a wide variety of charge distributions, such as the net or natural atomic charge [16], the Löwdin charge, etc.

Consider that the total amount of electrons Q_α on the element α are equally distributed on all the α atoms. Therefore, each element α will have an additional charge: $q_\alpha = Q_\alpha/n_\alpha$, which can be positive or negative. This value will depend on the relative electronegativity value with respect to the other atoms [17]. Now, instead of an integer number of elements n_α of the atom α, we have a fractional number of atoms given by

$$n'_\alpha = n_\alpha - \frac{q_\alpha}{\nu_\alpha^{\text{CDW}}} \tag{12}$$

In the case of neutral atoms, $q_\alpha = 0$ and we recover $n'_\alpha = n_\alpha$, as it should be.

To inspect the effect of q_α, we computed the molecular structure of several nucleobases with the GAMESS code. We used the 6-31G(d,p) basis set, which includes polarization functions for all the atoms. The calculations were carried out implementing the B3LYP functional [18, 19] to account for the correlation and exchange effects. In Table 2, we display the charge q_α of four DNA molecules. The last column shows the new stoichiometric formula found by implementing Eq. (12).

Element	C	H	N	O	New stoichiometry
Adenine	+0.32	+0.23	−0.55		$C_{4.92}H_{4.77}N_{5.14}$
Cytosine	+0.28	+0.21	−0.56	−0.53	$C_{3.93}H_{2.79}N_{5.14}O_{1.13}$
Guanine	+0.46	+0.20	−0.58	−0.36	$C_{4.89}H_{4.80}N_{5.15}O_{1.09}$
Thymine	+0.20	+0.19	−0.54	−0.52	$C_{4.95}H_{1.95}N_{6.13}O_{2.13}$

Table 2: Effective charge q_α and new stoichiometric formula defined by Eq. (12) for four DNA molecules.

The previous formula can be rewritten by replacing the integer value n_α by the fractional values n'_α. This analog formulations are now implemented to compute the new ionization cross sections, σ'.

In Figure 8, we display the relative difference of ionization cross sections

$$e = \frac{\sigma' - \sigma}{\sigma} \times 100 \tag{13}$$

for the four DNA bases. The difference obtained is of just very few percents, which indicates that the SSM is a quite robust model to treat the type of

molecule we are dealing with, and of course within the range error that one can expect from the SSM.

Our molecular binding energies of the outer electrons for adenine, cytosine, guanine and thymine are shown in Figure 7. On the left side of the figure, we show the atomic Hartree–Fock energies of the constituent elements, which can give an idea of how the molecular levels distribute. A dashed line around -0.8 a.u. is drawn to separate in two the band levels of the outer electrons. The electrons in the molecular targets corresponding to the $2s$ of N and C in the atomic case are placed in a secondary gap. The lower levels of the secondary gap correspond to the oxygen. The number of electrons in the valence shell for all O would seem to be equal to 4, as previously setted by the scaling rule Eq. (6). The N case is not as straightfoward; the electrons that would correspond to the $2s$ are located just below the line. The $\nu_\alpha^{\mathrm{CDW}}$ value given for N would suggest that a significant amount of electron density from the secondary gap is shared with the valence band.
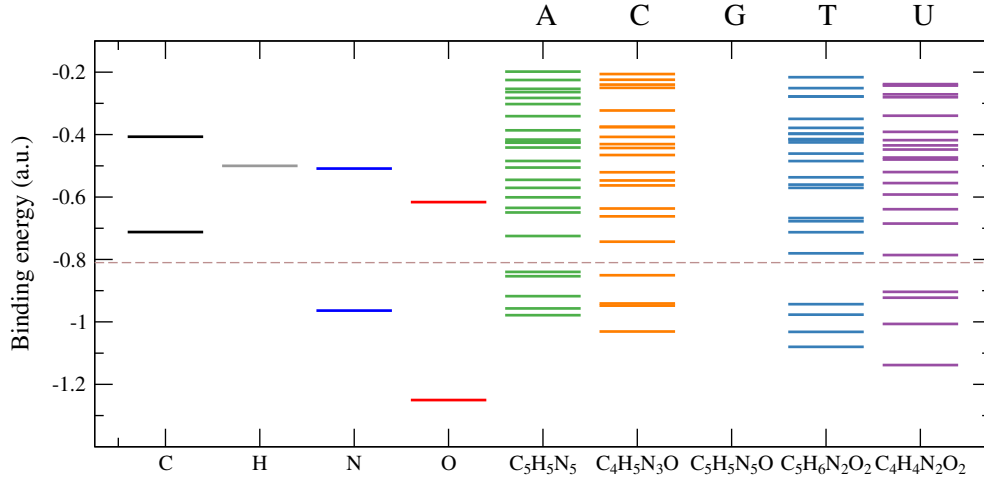
We now return to the calculation of the mean electron energy of H^+ and He^{2+} in water, $\overline{E}_{H_2O}$. If we consider that the residual charge of each hydrogen in water is $q_H = +0.35$ [17], which implies that on oxygen we have a residual charge of $q_O = -0.7$, we could re-write the formula of water using Eq. (13) as $H_{1.3}O_{1.17}$ by considering $n_O^{\mathrm{CDW}} \simeq 4$ and $n_H^{\mathrm{CDW}} \simeq 1$. Recalculating mean electron energy by impact of H^+ and He^{2+} on water at 1 MeV/amu, we obtain $\overline{E}_{H_2O} = 46.2$ and 47.6 eV. Our results are 10% apart from the experimental values: 51.5 and 52.2 eV [20], respectively, which is not bad considering the simplicity of our model.

Another parameter that can computed within our model is the fraction of energy carried by the electron f, which is defined as

$$f = \frac{\displaystyle\sum_\alpha n_\alpha \sigma_\alpha \overline{E_\alpha}}{\displaystyle\sum_\alpha n_\alpha (\sigma_\alpha \overline{E_\alpha} + \sum_{nl} \sigma_{\alpha nl} E_{\alpha nl})} \ . \tag{14}$$

Using our shell-to-shell ionization cross sections $\sigma_{\alpha nl}$ [7], and atomic binding energies of the atom α, $E_{\alpha nl}$ [22], we obtain $f = 0.70$ and 0.71 on water at 1 MeV/amu for H^+ and He^{2+}, which differ from the respective experimental values $f = 0.81$ and 0.80.

The difference between our calculations and the experiments could be attributed to the binding energy values of the molecular water 12.65 eV and its atomic components, H (13.6 eV) and O (17.19 eV). This theoretical discrepancy goes beyond our independent atom approximation and so it cannot be accounted for by our model. Once again, we could estimate this contribution by resorting to the stoichiometric model. We can make an asses for a maximum difference per molecule of water as

$$\delta E = (13.6 - 12.65) \times 1.17 + (17.19 - 12.65) \times 1.3 = 7 \, \text{eV} \tag{15}$$

Most of this energy should be transfer to the kinetic energy of the emitted electron. Thus, by adding 7 eV to the previous values, we obtain $\overline{E}_{H_2O} = 53.2$ and 54.6 eV for H^+ and He^{2+} on water at 1 MeV/amu, respectively, which are much closer to the experimental values. If we add δE to the numerator of Eq. (14), we obtain $f = 0.81$ and 0.80, in perfect agreement with the experiments (see Table 1 of Ref. [20]).

4   Conclusions

We calculated ionization cross sections by impact of antiprotons, H^+, He^{2+}, Be^{4+}, C^{6+}, and O^{8+} for sixteen molecules containing H, C, N, O, P and S with the CDW method. The importance of the influence of Z was observed in the mean energy $\overline{E}_\alpha$ and angle $\overline{\theta}_\alpha$. For a given target α, as Z increases, $\overline{E}_\alpha$ increases, but $\overline{\theta}_\alpha$ decreases. At high impact energy, say larger than 1 MeV/amu, these values converge to the Born approximation, which embodies the simple Z^2 law. The sixteen molecules selected were investigated using the simple stoichiometric model. Results for six DNA bases were presented

and compared with the sparse available experiments. We explore the rule of Toburen which scales all the molecular ionization cross section when divided by the number of weakly bound valence electrons ν_α given by Eq. (2). We found the rule scales much better when normalizing our theoretical ionization cross sections to the number $\nu_\alpha^{\mathrm{CDW}}$ given by Eq. (6). Finally, we attempt to improve the stoichiometric model by using the Mulliken charge to define a new model containing fractional rather than integer proportions. No substantial correction was found, which indicates that the SSM works quite well. By inspecting the molecular binding energy from quantum mechanical structure calculations, we were able to understand the values defined for $\nu_\alpha^{\mathrm{CDW}}$.

The main objective of this article is to provide the tools to estimate any inelastic parameter parameter –such as emission angle, emitted mean energy and cross section– by the impact of any multicharged on any molecule containing H, C, N, O, P and S, with the help of the stoichimetrical model. Our goal was quite ambitious, considering the simplicity of our proposal. However, we think our results could be used to estimate the ionization magnitude with an acceptable level of uncertainty.

References

[1] M. W. Schmidt, K. K. Baldridge, J. A. Boatz, S. T. Elbert, M. S. Gordon, J. H. Jensen, S. Koseki, N. Matsunaga, K. A. Nguyen, S. J. Su, T. L. Windus, M. Dupuis, J. A. Montgomery J. Comput. Chem. 14, 1347-1363 (1993)

[2] J. E. Miraglia and M. S. Gravielle. Ionization of the He, Ne, Ar, Kr, and Xe isoelectronic series by proton impact. Phys Rev A **78**, 052705 (2008)

[3] J. E. Miraglia, Ionization of He, Ne, Ar, Kr, and Xe by proton impact: Single differential distributions. Phys Rev A **79**, 022708 (2009).

[4] A.M.P. Mendez, D.M. Mitnik, and J.E. Miraglia. Depurated inversion method for orbital-specific exchange potentials. Int. J. Quantum Chem. 24 ,116 (2016).

[5] A.M.P. Mendez, D.M. Mitnik, and J.E. Miraglia. Local Effective Hartree–Fock Potentials Obtained by the Depurated Inversion Method, 76. (2018).

[6] Ionization probabilities of Ne, Ar, Kr, and Xe by proton impact for different initial states and impact energies. Nucl. Instr. Meth. Phys. Res. B 407 (2017) 236-243.

[7] J. E. Miraglia. Shell-to-shell ionization cross sections of antiprotons, H^+, He^{2+}, Be^{4+}, C^{6+} and O^{8+} on H, C, N, O, P, and S atoms To be published Archive 2019.

[8] A. Itoh, Y. Iriki, M. Imai, C. Champion, and R. D. Rivarola, Cross sections for ionization of uracil by MeV-energy-proton impact, Physical Review A 88, 052711 (2013)

[9] in energy and angles ,

[10] C Champion, M E Galassi, O Fojón, H Lekadir, J Hanssen, R D Rivarola, P F Weck, A N Agnihotri, S Nandi, and L C Tribedi. Ionization of RNA-uracil by highly charged carbon ions. J. Phys.: Conf. Ser. 373, 012004 (2012).

[11] A. N. Agnihotri, S. Kasthurirangan, S. Nandi, A. Kumar, M. E. Galassi, R. D. Rivarola, O. Fojón, C. Champion, J. Hanssen, H. Lekadir, P. F. Weck, and L. C. Tribedi. Ionization of uracil in collisions with highly charged carbon and oxygen ions of energy 100 keV to 78 MeV. Phys Rev A 85, 032711 (2012).

[12] W. E. Wilson and L. H. Toburen. Electron emission from proton — hydrocarbon-molecule collisions at 0.3—2.0 MeV. PHYSICAL REVIEW A 11 1303 (1975).

[13] D. J. Lynch, L. H. Toburen, and W. E. Wilson. Electron emission from methane, ammonia, monomethylamine, and dimethylamine by 0.25 to 2.0 MeV protons. J. Chem. Phys. 64, 2616 (1976).

[14] Multiscale approach to the physics of radiation damage with ions. E. Surdutovich and A. V. Solov'yov, arXiv:1312.0897v, (2013)

[15] P. de Vera1, I. Abril, R. Garcia-Molina and A.V.Solov'yov, Ionization of biomolecular targets by ion impact: input data for radiobiological applications. Journal of Physics: Conference Series 438 (2013) 012015

[16] Jung-Goo Lee, Ho Young Jeong, and Hosull Lee, Charges of Large Molecules Using Reassociation of Fragments. Bull. Korean Chem. Soc.24 2003, 369 .

[17] A. K. Rappe, A. K.and W. A. Goddard III,. J. Phys. Chem. **95** (1991) 3358.

[18] A. D. Becke, J. Chem. Phys. 98, 5648-5652 (1993)

[19] P. J. Stephens, F. J. Devlin, C. F. Chabalowski, M. J. Frisch, J. Phys. Chem. 98, 11623-11627 (1994)

[20] S.M. Pimblott and J. A. LaVerne, Radiation Physics and Chemistry 76, 1244-1247 (2007)

[21] M. E. Rudd, Y.-K. Kim,, D. H. Madison and T. J. Gay. Electron production in proton collisions with atoms and molecules: energy distributions. Rev. Mod. Phys. **64**, 44-490 (1992).

[22] E. Clementi, C. Roetti, At. Data Nucl. Data Tables 14, 177–478 (1974).